Analysis of an HCDA in the SNR-300 using the code SEURBNUK/EURDYN

A.Yerkess

Commission of the European Communities, Joint Research Centre, Ispra Establishment, Italy

E.S.Meier

Gesellschaft für Reaktorsicherheit (GRS) mgH, Köln, FR Germany

1 INTRODUCTION

For the SNR-300 prototype fast reactor, a numerical simulation of the loading of the primary containment undergoing a Hypothetical Core Disruptive Accident (HCDA) with a mechanical release of 370 MJ had to be analysed using a well-proven fluid dynamics/structural code. In the past, the code SEURBNUK-2 /1,2,3/, has been adequately validated using data from many experimental scaled-model tests /4/, and analytic solutions /5/. In particular, SEURBNUK-2 was used to analyse an HCDA simulation in a 1/6 scaled-model of the SNR-300 /6/, and therefore it was deemed to be a natural choice for the full-scale analysis.

In parallel to the SEURBNUK development, the coupled code SEURBNUK-EURDYN release 1 /7/ has also evolved. The finite element code EURDYN01 /8/ is a substitute for the built-in thin shell finite difference scheme available in SEURBNUK and it allows for better modelling of thick structures and structural inter-connectivity. Since SEURBNUK-2 and SEURBNUK/EURDYN were at the same level of development, both codes were used in the SNR-300 analysis and their structural responses compared.

2 THE STRUCTURAL DESIGN OF THE REACTOR VESSEL

The cylindrical primary vessel with a hemispherical bottom, diameter 6.7 m and total length 14.0 m, hangs by means of a flange fixed to the support platform, see Fig. 1. Sodium coolant inlet and outlet pipes, connected to three separate secondary circuits containing pumps and heat exchangers, are welded radially into the upper section of the primary vessel at equal circumferential intervals.

Immediately on entry into the primary vessel, the sodium coolant inlet pipes bend vertically downwards and are connected to the inlet plenum, diameter 3.9 m, whose base curvature follows closely that of the primary vessel. The diagrid, centrally perforated to allow coolant flow through the core, forms the upper boundary of the inlet plenum. On the upper surface of the diagrid, positioned by means of inserts, rests the core which is made up of fissile, breeder, blanket and adsorber assemblies. The shield tank, diameter 4.6 m and length 6.4 m, is connected by means of a conical attachment to the outer circumference of the diagrid which, in turn, is fixed to a cylindrical core support welded at its bottom end to the primary vessel. The sodium which overflows into the outer annular zone is transported by the three outlet pipes to the secondary circuit intermediate heat exchangers.

Approximately 0.3 m above the top edge of the shield tank is a circular perforated dip-plate supported by means of columns and an external cylindrical shell to the reactor roof which also supports the control rods and emergency cooling circuits. The composite roof structure, diameter about 7.0 m and thickness 3.3 m, contains a three-plug rotating mechanism, the two smallest plugs being eccentrically regulated by the largest one during the re-fuelling process. The complex roof structure with seals forms the closure to the vessel and is bolted down to the support platform which is firmly implanted in the re-inforced concrete floor of the reactor building.

3 MODELLING OF THE REACTOR VESSEL AND ITS COMPONENTS

The codes used to model the reactor response to an HCDA are axisymmetrically formulated and with them it is not possible to model precisely 3-D structures. However, in many cases 2-D equivalents suffice, or when 3-D effects are localized or negligible, they can be omitted. The sodium coolant pipes are considered the most important components subject to this limitation but due to difficulties in realizing a 2-D equivalent they have not been modelled.

The spherical bottom of the primary vessel is uniformly thick (60 mm) whereas in the cylindrical section the thickness is variable (37-40 mm) (see Fig. 2). The shield tank, made up of two concentric shells separated by a 50 mm wide fissure, is modelled as a unique shell, thickness 70 mm, which is augmented to 87 mm in the lower half to include the effect of the core blanket.

Fluid flow to and from the hemispherical-bottomed, cylindrical inlet plenum, uniform thickness 40 mm, is realized via perforations in the digrid from which it is suspended. The intervening space between the inlet plenum, the core support and the base of the primary vessel is larger than in reality due to code limitations. The cylindrical core support, thickness 60 mm, is interrupted along its length by a perforated area, thickness 50 mm, to account for both area and weakness caused by the sodium inlet pipes. The diagrid, whose mass includes the inserts, the core support guard-plate flange and the inlet plenum flange, is simulated as a deformable thin shell, thickness 0.23 m, perforated up to radius 0.785 m.

The perforated dip-plate (perforation ratio 0.2) has two thicknesses, 100 mm up to radius 1.26 m and 120 mm thereafter. The dip-plate support is simulated by three concentric thin shells, the transverse fluid flow being unimpeded. The reactor roof, thickness 0.2 m, is held down by bolts modelled as an equivalent cylindrical shell. The response of the reactor support platform is considered stationary. Due to the fact that SEURBNUK cannot resolve the motion of two independent parallel shells in very close proximity, the thermal shock plate attached at its lower end to the primary vessel has been omitted. The hoop strain of the primary vessel is thus clearly overestimated.

Surrounding the fissile zone (modelled in run 4 only) is a cylindrical can, diameter 3.0 m, thickness 0.1 m, which simulates the composite breeder/reflector zone. The material is considered almost ideally plastic with a low yield strength.

Although the thick structures (e.g. the roof and diagrid) could have been modelled by SEURBNUK/EURDYN as being thick, in fact they were modelled as thin shells so that direct comparisons could be made with SEURBNUK-2 results. The thickness of the roof, diagrid and the breeder/reflector zone reported above are artificial, however, their densities and Young's moduli are appropriately increased in order to obtain correct masses and rigidities. Using this numerical manipulation the stability time step for these structures can be usefully increased to reduce CPU time.

The reaction zone formed by the hypothetical core disruption is initially assumed to be cylindrical, diameter 1.57 m, height 0.96 m, and its expansion is described by a tabular pressure-volume (p-v) curve which basically follows the relationship, $pv^{\gamma} = \text{constant}$, where the polytropic gas exponent is a function of the volume and varies from 0.2 to 1.1. With an initial pressure of 24 MPa and a final volume of about 70 m^3, the resulting energy release is 370 MJ. An ideal gas equation is used to describe the cover gas behaviour, and the sodium coolant is described by a simple 2-D equation based on a knowledge of the Huguniot shock data.

4 THE SEURBNUK-2 AND SEURBNUK/EURDYN CODES

SEURBNUK-2 and SEURBNUK/EURDYN are both 2-D axisymmtric fluid dynamic codes which use an implicit finite difference algorithm similar to ICE /9/, to compute the fluid motion. For the structural computation SEURBNUK has a built-in finite difference thin shell model, whereas SEURBNUK/EURDYN is coupled to the finite element code EURDYN01 whose 3-node triangular element has the added advantage of adequately modelling many thick structures found in reactors. The ad hoc "stiff junction" used to connect structures in SEURBNUK, although proved adequate in many problems, is not as ideal as the more rigorous approach available in EURDYN01.

The fluid-structure coupling algorithm for both codes is semi-implicit, that is, the formulation implicitly connects the fluid and structure calculations for the pressure derived forces, while the internal structural and body forces are treated explicitly /10/. Hence, the coupling in SEURBNUK/EURDYN is now "stronger" than the explicit "weak" coupling existing in earlier versions and leads to better stability. Since the stability step for the fluid is generally larger than that of the structures, a subcycling technique is adopted to increase computing efficiency.

Other recent improvements to the codes such as an automatic bubble rezoning facility to smooth out numerical perturbations, an extended logic for multifluid cells, a simplified logic to describe structural boundaries and automatic finite element generation have achieved substantially better program performance with a doubling of the final time reached in the case of these SNR-300 calculations.

5 RESULTS

Four calculations were performed. Runs 1 and 2 have identical input data and are calculated using codes SEURBNUK-2 and SEURBNUK/EURDYN, respectively. Run 3 is similar to run 2 but with modified material data for the shield and primary tanks, and run 4 is similar to run 1 but with a structure surrounding the reaction zone to simulate the composite breeder/reflector zone. All structures, except in run 4, experience similar pressure loading scenarios. A brief review of some of the more important events will be described.

First, the shield tank and the primary vessel undergo structural deformation at the height of the core due to the initial pressure wave. Since the upper end of the shield tank is free, the positive hoop strain is accompanied by an axial contraction. The hoop and axial strains for the primary vessel are both positive, the axial strain being further augmented when the loading on the diagrid is transferred to it via the core support. Up to 15 ms the fluid movement is omnidirectional, but thereafter it is dominantly upwards and further loads the head and hold-down bolts via transmission through the dip-plate and its support. As the reaction zone expands, fluid is forced through the gap between the top of the shield tank and the dip-plate into the outer annular zone and proceeds towards the roof. Fig. 3 shows a graphical snapshot at 48 ms.

Comparison between run 1 (SEURBNUK-2) and run 2 (SEURBNUK/EURDYN) reveals the following general observations. The impulses all along the shield tank for run 2 are slightly higher, see Fig. 4, the maximum difference being about 5% close to the free end. However, the corresponding strains were lower, see Fig. 5, by about 10-15%. The agreement obtained for pressure loading on the outer tank varies according to position, with greater divergence in the upper half of the vessel. Although the agreement for impulses at charge height is good, see Fig. 6, the corresponding comparison in strains is less favourable, see Fig. 7. The final strains of the primary vessel above the dip-plate level are actually greater in run 2. A simple comparison of code responses for the primary vessel cannot be made as they are also influenced by the transmission of axial loads to the primary vessel via the diagrid and core support. A change in gap size between the dip-plate and the top of the shield tank due to the downward motion of the diagrid will also affect the fluid flow through this gap up towards the roof.

It is difficult to determine which set of results are more correct. The inter-structural connectivity is obviously better in ERUDYN because of the more accurate modelling of end constraints, on the other hand, EURDYN underestimates the calculation of large strains due to its small strain limitation. The point of pressure load application is also slightly different, for EURDYN it is at the external surface of the shell and for SEURBNUK it is at the mid-surface. Furthermore, SEURBNUK used the mechanical sub-layer model, whereas EURDYN used the isotropic strain hardening model to describe the strain hardening effect. Although it is intuitively felt that the EURDYN results are more correct, nevertheless it is comforting to have such close agreement.

Figs. 8a and 8b indicate the different temperature distributions close to the core region for the primary vessel and shield tank, respectively. Changing the material properties of the shield tank and the primary vessel to take into account the temperature changes has only influenced the results in these localized areas. The net hardening of the materials in run 3 has led to negligible decreases in the strains for the shield tank and a decrease of approximately 8% in the hoop strains at charge height for the primary vessel.

Run 4, a SEURBNUK run which also simulates the breeder/reflector zone, only ran until 23 ms due to a code limitation concerning parallel shell proximity. It is clear that in run 4 some of the available energy must be used to accelerate and deform the breeder/reflector zone, thus the energy remaining to deform the other structures is substantially reduced. Figs. 9 and 10 indicate how the strains on the shield tank and primary vessel are affected by its inclusion.

6 CONCLUSIONS

The comparison between SEURBNUK-2 and SEURBNUK/EURDYN results shows that the responses are similar, and in general it is thought that the SEURBNUK/EURDYN results are marginally better. Changing the material properties to take into account the two specific temperature distributions in the vicinity of the core produced small localized differences in the vessel strains. The inclusion of the breeder/reflector zone substantially reduced the vessel strains. Even in the least favourable case considered, the predicted structural responses indicate that good containment capabilities are assured.

7 REFERENCES

1. Cameron et al. 1977. The computer code SEURBNUK-2 for fast reactor containment studies. Paper B2/1, SMiRT-4, San Francisco.
2. Staniforth, R. & Yerkess, A. 1979. The computer code SEURBNUK-2: recent developments. Paper E1/1, SMiRT-5, Berlin.
3. Smith, B.L., Yerkess, A. & Adamson, J. 1983. Status of the coupled fluid-structure code SEURBNUK. Paper B9/1, SMiRT-7, Chicago.
4. Albertini, C. et al. The JRC-COVA programme: final report. EUR 8705e.
5. West, P.L. & Hoskin, N.E. 1980. APRICOT - phase 3. Suggested simple test problems for examination of thin shell modelling and fluid structure coupling. Aldermaston report AWRE/44/92/16.
6. Meier, E.S., Smith, B.L. & Yerkess, A. 1981. Analysis of the HCDA - simulation in a 1/6th-scaled model of the SNR-300 with the SEURBNUK-2 code. Paper E3/3, SMiRT-6, Paris.
7. Smith, B.L., Yerkess, A. & Washby, V. 1987. The computer code SEURBNUK-EURDYN: first release version. Paper E6/6, SMiRT-9, Lausanne.
8. Donea, J. & Giuliani, S. 1975. EURDYN, finite element codes for dynamic analysis of large displacement, small strain problems with material non-linearities. Paper M2/5, SMiRT-3, London.
9. Harlow, F.H. & Amsden, A.A. 1971. A numerical fluid dynamics calculation method for all speeds. J. Comp. Phys., 8.
10. Smith, B.L. 1985. A new fluid/structure coupling algorithm for the LMFBR containment code SEURBNUK/EURDYN. Paper B2/6, SMiRT-8, Brussels.

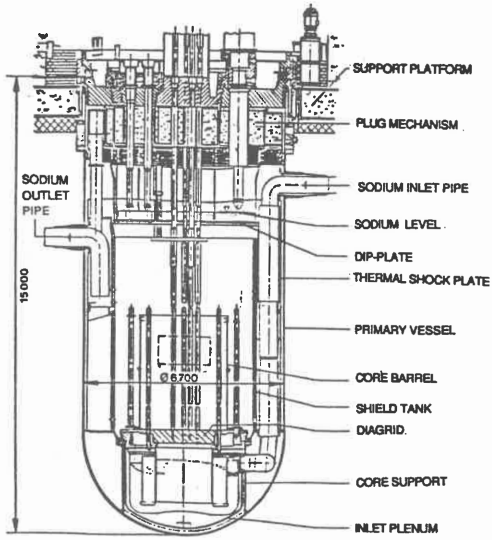

Fig. 1 SNR-300 primary vessel with internals.

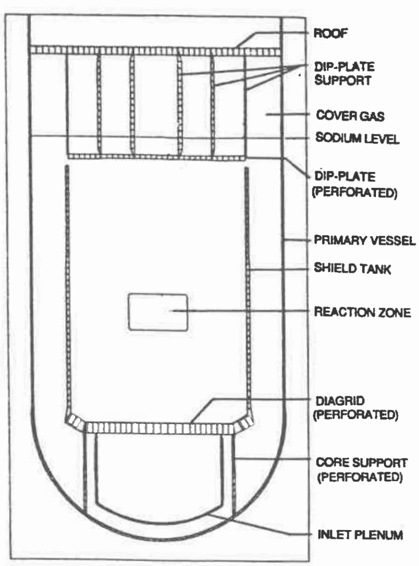

Fig. 2 Simulation model of the SNR-300.

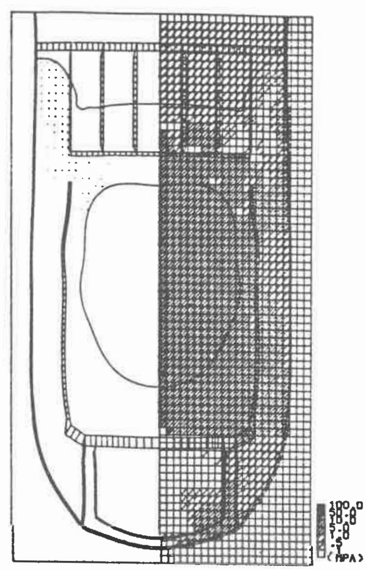

Fig. 3 SEURBNUK/EURDYN configuration at 48 ms.

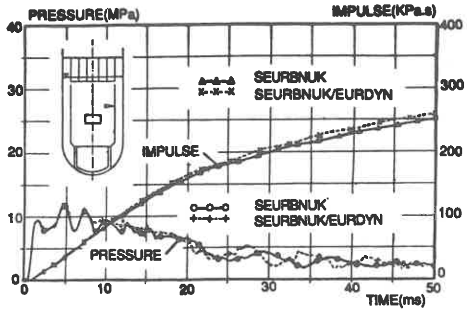

Fig. 4 Pressures and impulses
- shield tank.

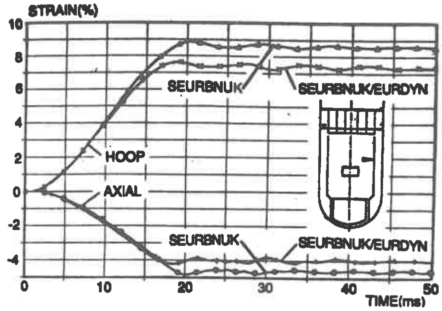

Fig. 5 Hoop and axial strains
- shield tank.

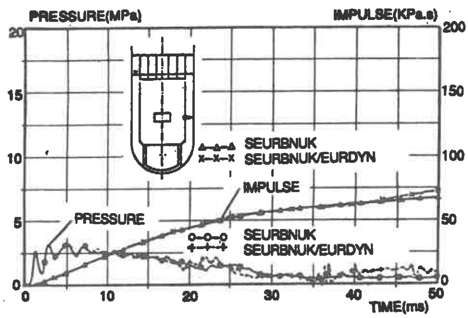

Fig. 6 Pressures and impulses
- primary vessel.

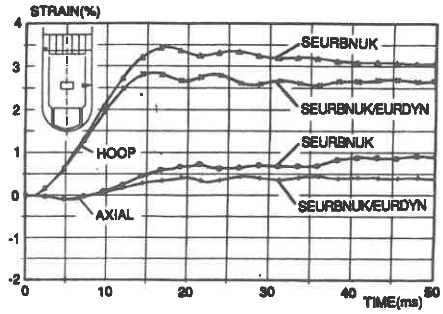

Fig. 7 Hoop and axial strains
- primary vessel.

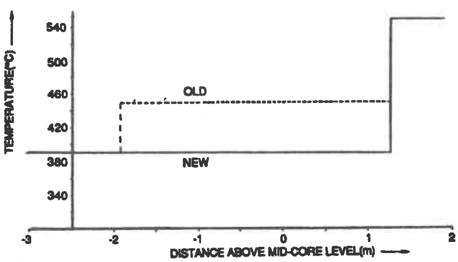

Fig. 8a Temperature distribution
- shield tank

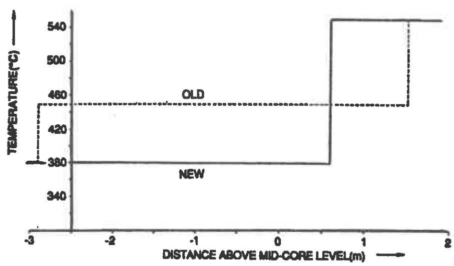

Fig. 8b Temperature distribution
- primary vessel

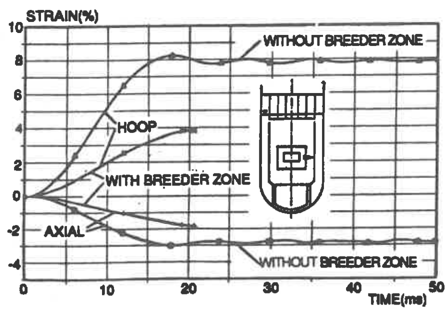

Fig. 9 Hoop and axial strains
- shield tank.

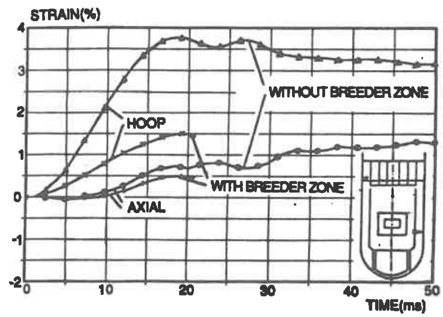

Fig. 10 Hoop and axial strains
- primary vessel.